ISSN 1070-3284, Russian Journal of Coordination Chemistry, 2017, Vol. 43, No. 3, pp. 156–163. © Pleiades Publishing, Ltd., 2017.
Original Russian Text © D.A. Garnovskii, S.I. Levchenkov, G.G. Aleksandrov, V.G. Vlasenko, Ya.V. Zubavichus, A.I. Uraev, A.S. Burlov, 2017, published in Koordinatsionnaya Khimiya, 2017, Vol. 43, No. 3, pp. 147–155.

Electrochemical Synthesis, Properties, and Structure of Copper, Nickel, and Cobalt Complexes of Tridentate Tosylamino-Functionalized Mercaptopyrazole Schiff Base

D. A. Garnovskii[a], *, S. I. Levchenkov[a], G. G. Aleksandrov[b], †, V. G. Vlasenko[c], Ya. V. Zubavichus[d], A. I. Uraev[e], and A. S. Burlov[e]

[a] *Southern Scientific Center, Russian Academy of Sciences, ul. Chekhova 41, Rostov-on-Don, 344006 Russia*
[b] *Kurnakov Institute of General and Inorganic Chemistry, Russian Academy of Sciences, Leninskii pr. 31, Moscow, 117907 Russia*
[c] *Research Institute of Physics, Southern Federal University, ul. Stachki 194, Rostov-on-Don, 344090 Russia*
[d] *National Research Center "Kurchatov Institute", pl. Akademika Kurchatova 1, Moscow, 123182 Russia*
[e] *Institute of Physical and Organic Chemistry, Southern Federal University, ul. Stachki 194/2, Rostov-on-Don, 344090 Russia*
**e-mail: garn@ipoc.sfedu.ru*

Received May 10, 2016

Abstract—Copper, nickel, and cobalt complexes of the N,N,S-tridentate tosylamino-functionalized mercaptopyrazole Schiff base were obtained by an electrochemical method. The structure and composition of the metal chelates were characterized by C, H, N elemental analysis data and IR and ^{1}H NMR spectroscopy. More data on the structures of the complexes were obtained by magnetochemical and X-ray absorption spectroscopy measurements. The mononuclear structure of the copper(II) complex was confirmed by X-ray diffraction (CIF file CCDC no. 1473320).

Keywords: electrochemical synthesis, tridentate Schiff base, metal chelates, binuclear copper complex, X-ray diffraction

DOI: 10.1134/S1070328417030010

INTRODUCTION

The complexes of tridentate aromatic Schiff bases derived from 2-tosylaminoaniline with various combinations of N,O-donor centers in the chelate unit attract permanent attention due to the possibility to vary composition, structure, and properties of the complexes depending on the central ion and ligand environment.

Using electrochemical method [1, 2] binuclear complexes of H_2L^1 with various 3d metals with ferro- and antiferromagnetic exchange interactions were synthesized [3–6].

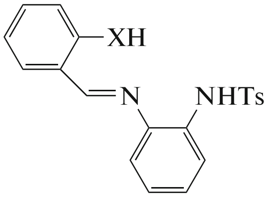

H_2L^1: X = O and H_2L^2: X = NTs

Adducts [$ML^2 \cdot L'$] (M = Co(II), Ni(II), Zn(II), L' = 2-aminopyridine; M = Cu(II), L' = CH_3OH) based on H_2L^2 have been prepared by the electrochemical method and structurally characterized [7, 8]. Mononuclear metal chelates [ML^2] [9], M = Ni(II), Cu(II), with rarely encountered bond between the metal and the oxygen of tosyl group, and their adducts with 2,2'-bipyridine, 1,10-phenanthroline, and 1,1-diphenylphosphanylmethane have been prepared in acetonitrile. The introduction of a heterocyclic hydroxypyrazole moiety into the tosylamino-functionalized Schiff base may give both polymeric products owing to coordination to the pyridine type nitrogen of the pyrazole moiety (in the case of zinc) and mononuclear complexes with various geometries of the MN_2O_2 or MN_3O chelate unit, M = Cu(II), Ni(II), Co(II) [10, 11].

This paper is devoted to the electrochemical synthesis and study of physicochemical properties and structures of copper(II) (**I**), nickel(II) (**II**), and cobalt(II) (**III**) complexes with tridentate N,N,S-sulfonamide pyrazole azomethine derivatives.

---

† Deceased.

EXPERIMENTAL

1-Phenyl-3-methyl-4-formylpyrazole-5-thiol and 2-tosylaminoaniline were synthesized according to the published methods [12] and [13].

Synthesis of *N*-[2-[[3-methyl-1-phenyl-5-thioxopyrazol-4-ylidenemethyl]amino]phenyl]-4-methylbenzenesulfonamide (H_2L). A solution of 2-tosylaminoaniline (1.05 g, 0.004 mol) in 10 mL of ethanol was added to a solution of 1-phenyl-3-methyl-4-formylpyrazole-5-thiol (0.87 g, 0.004 mol) in 10 mL of ethanol. The reaction mixture was refluxed for 2 h. The bright orange crystals that precipitated on cooling were collected on a filter, washed with 10 mL of hot 2-propanol, and dried in vacuum. The yield of orange crystals was 1.55 g (89%). T_m = 171–172°C.

For $C_{24}H_{22}N_4O_2S_2$			
anal. calcd., %:	C, 62.34;	H, 4.76;	N, 12.12.
Found, %:	C, 62.19;	H, 4.75;	N, 12.07.

IR (KBr; ν, cm^{-1}): 3183 w ν(N–H), 1638 s ν(C(=S)CH=CHN–), 1324 s $\nu_{as}(SO_2)$, 1154 s $\nu_s(SO_2)$.

^{1}H NMR (DMSO-d_6; δ, ppm): 2.40 (s, 3H, CH_3), 2.43 (s, 3H, CH_3), 6.68–8.04 (m, $13H_{arom}$), 8.67 (d, 1H, C*H*–NH, ^3J = 12.4 Hz), 9.89 (s, 1H, N–H), 14.49 (d, 1H, CH–N*H*, ^3J = 12.4 Hz).

Electrochemical synthesis of the complexes was carried out by the standard classical procedure [14] using a EG&GPAR/173 potentiostat in a methanol–acetonitrile (1 : 1) solution with a platinum cathode and a metal (Ni, Co, Cu) plate as the anode. The working solution (25 mL) contained 0.001 mol of H_2L and 0.01 g of Et_4NClO_4 as the electrolyte. The electrolyses were carried out in an undivided U-shaped glass tube at a 15 mA current and initial voltage of 12 V for 1.5 h. After completion of the electrolises, the precipitates of the complexes were filtered off, washed with hot 2-propanol, and dried in vacuum.

Complex **I**: brown crystals. Yield 0.087 g (65%). T_m = 198–199°C.

For $C_{25}H_{24}N_4O_3S_2Cu$			
anal. calcd., %:	C, 53.95;	H, 4.32;	N, 10.07.
Found, %:	C, 53.84;	H, 4.39;	N, 10.14.

IR (KBr; ν, cm^{-1}): 1603 s ν(C=N), 1237 s $\nu_{as}(SO_2)$, 1115 s $\nu_s(SO_2)$.

The single crystals of complex **I** for X-ray diffraction were obtained by recrystallization from a methanol–acetonitrile solution (1 : 1).

Complex **II**: brown crystals. Yield 0.076 g (57%). T_m = 203–204°C.

For $C_{25}H_{24}N_4O_3S_2Ni$			
anal. calcd., %:	C, 54.54;	H, 4.36;	N, 10.18.
Found, %:	C, 54.49;	H, 4.27;	N, 10.11.

IR (KBr; ν, cm^{-1}): 1604 s ν(C=N), 1248 s $\nu_{as}(SO_2)$, 1138 s $\nu_s(SO_2)$. ^{1}H NMR (DMSO-d_6; δ, ppm): 2.31 (s, 3H, CH_3), 2.44 (s, 3H, CH_3), 3.21 (d, 3H, C*H*$_3$OH, ^3J = 6.7 Hz), 4.05(q,1H, CH_3O*H*, ^3J = 6.7 Hz), 6.87–7.94 (m, $13H_{arom}$), 8.86 (s, 1H, CH=N).

Complex **III**: brown crystals. Yield 0.081 g (61%). T_m = 207–208°C.

For $C_{52}H_{56}N_8O_8S_4Co_2$			
anal. calcd., %:	C, 56.37;	H, 5.06;	N, 10.12.
Found, %:	C, 56.69;	H, 4.98;	N, 10.23.

IR (KBr; ν, cm^{-1}): 1606 s ν(C=N), 1252 s $\nu_{as}(SO_2)$, 1137 s $\nu_s(SO_2)$.

C,H,N-elemental analysis was performed on a TCM 480 Carlo Erba Instruments analalyzer. The IR spectra of the samples as KBr pellets were measured on a Nicolet Impact-400 instrument in the 4000–400 cm^{-1} range. ^{1}H NMR spectra were recorded on a Varian Unity 300 spectrometer operating at 300 MHz with 2H internal lock in DMSO-d_6 at 20°C. The specific magnetic susceptibility was determined by the relative Faraday method in the 77.4–300 K range; $Hg[Co(CNS)_4]$ was used as the calibration standard. The melting point was determined on a Koefler table.

X-ray absorption spectroscopy. Cu, Co, and Ni *K*-edge X-ray absorption spectra of compounds **I–III** were recorded at a Structural Materials Science station of the Kurchatov synchrotron radiation source (Moscow) [15]. The energy of the electron beam used as the source of X-ray synchrotron radiation was 2.5 GeV at a current of 60–80 mA. The X-ray radiation was monochromatized using a double-crystal monochromator with a Si(111) single crystal slit. The X-ray beam intensity before and after sample irradiation was determined using two ionization chambers filled with nitrogen–argon mixtures providing 20 and 80% absorption for I_0 and I_t, respectively. The obtained X-ray absorption spectra were treated with standard procedures of background subtraction, normalization to the *K*-edge step, and isolation of atomic absorption μ_0 [16]; after this, the resulting EXAFS χ-spectra were Fourier-transformed in the range of photoelectron wave vectors *k* from 2.6 to 12–13 Å^{-1} with the weight function k^3. The obtained Fourier transform moduli (FTM) of EXAFS corresponded, to an accuracy of phase shift, to the atomic radial distribution function around the absorbing metal atom. The threshold ionization energy (E_0) was chosen from the maximum of the K-edge first derivative and subsequently varied for fitting.

The exact parameters of the local environment of the absorbing metal atoms in the complexes were determined by non-linear fitting of the coordination sphere parameters by comparison of the simulated EXAFS spectrum with that isolated from the full χ-spectrum by Fourier filtration. This non-linear fitting was performed using the IFFEFIT program package [17]. The photoelectron wave scattering phases and amplitudes needed for the calculation of the model spectrum were calculated by the FEFF7 program [18]. The single crystal X-ray diffraction data for complexes with a similar atomic environment of metal ions were used as the initial atomic coordinates needed to calculate the scattering phases and amplitudes and for the subsequent fitting. The structures of such complexes were retrieved from the Cambridge Crystallographic Data Centre.

The number of parameters varied during the multisphere fitting did not exceed, in all cases, the number of independent parameters N_{ind}, which can be reliably determined from the EXAFS spectrum in the specified ranges Δk and Δr using formula (1):

$$N_{\text{ind}} = (2\Delta r\Delta k/\pi) + 1, \qquad (1)$$

where Δk is the analyzed EXAFS spectrum region in the space of photolelectron wave vectors, Δr is the R-space region in which the Fourier filtration is performed.

During fitting, the following function was minimized (2) :

$$\chi^2 = \frac{N_{\text{ind}}}{N_{\text{pts}}\varepsilon^2}\sum_{i=1}^{N_{\text{pts}}}\Big\{[\mathrm{Re}(\tilde{\chi}_{\text{data}}(R_i) - \tilde{\chi}_{\text{th}}(R_i))]^2 + [\mathrm{Im}(\tilde{\chi}_{\text{data}}(R_i) - \tilde{\chi}_{\text{th}}(R_i))]\Big\}^2, \qquad (2)$$

where N_{pts} is the number of points in the fitting region. The absolute magnitude of the mean-square deviation between the simulated and experimental spectra was determined by the $\Re$-factor calculated from formula (3):

Table 1. Crystallographic data and X-ray experiment and structure refinement details for complex **I**

Parameter	Value
M	556.14
Crystal size, mm	0.43 × 0.18 × 0.09
Temperature of measurements, K	153(2)
System	Triclinic
Space group	$P\bar{1}$
a, Å	8.9627(5)
b, Å	10.1008(6)
c, Å	14.1367(8)
α, deg	89.0098(8)
β, deg	75.1448(8)
γ, deg	71.9583(8)
V, Å^3	1173.51(12)
Z	2
ρ(calcd.), g/cm^3	1.574
μ, mm^{-1}	1.146
F(000)	574
Scanning range of θ, deg	1.49–29.10
Ranges of reflection indices	$-12 \le h \le 12$, $-13 \le k \le 13$, $-19 \le l \le 19$
Number of measured reflections	12227
Number of unique reflections	6043
Number of reflections with $I > 2\sigma(I)$	5074
Number of refined parameters	322
GOOF (all reflections)	0.999
R_1 ($I > 2\sigma(I)$)	0.0364
wR_2 (all reflections)	0.1191
$\Delta\rho_{\max}/\Delta\rho_{\min}$, e Å^{-3}	0.801/–0.918

$$\Re = \sum_{i=1}^{N_{\text{pts}}}\frac{[\mathrm{Re}(\chi_{\text{data}}(R_i) - \chi_{\text{th}}(R_i))]^2 + [\mathrm{Im}(\chi_{\text{data}}(R_i) - \chi_{\text{th}}(R_i))]^2}{[\mathrm{Re}(\chi_{\text{data}}(R_i))]^2 + [\mathrm{Im}(\chi_{\text{data}}(R_i))]^2}. \qquad (3)$$

The X-ray diffraction analysis of complex **I** was carried out on an Agilent Technologies Xcalibur E diffractometer equipped with a CCD array detector and monochromatic radiation source (MoK_α, λ = 0.71073 Å) using the standard CrysAlisPro procedure [19]. The structure was solved by the direct method and refined in the full-matrix anisotropic approximation for all non-hydrogen atoms. The hydrogen atoms in **I** were located from the difference electron density maps and refined in the isotropic approximation. The key crystallographic data and structure refinement parameters for complex **I** are presented in Table 1. All calculations were carried out using the SHELXS-97 program package [20]. The full set of X-ray diffraction data is deposited with the Cambridge Crystallographic Data Centre (no. 1473320; deposit@ccdc.cam.ac.uk or http://www.ccdc.cam.ac.uk/data_request/cif).

RESULTS AND DISCUSSION

As a continuation of early studies [10, 11] dealing with the complexing ability of the tridentate hydroxypyrazole Schiff base with Zn^{2+}, Cu^{2+}, Co^{2+}, and Ni^{2+} ions, we carried out electrochemical synthesis of cobalt, nickel, and copper chelates with its sulfur analog (H_2L) (Scheme):

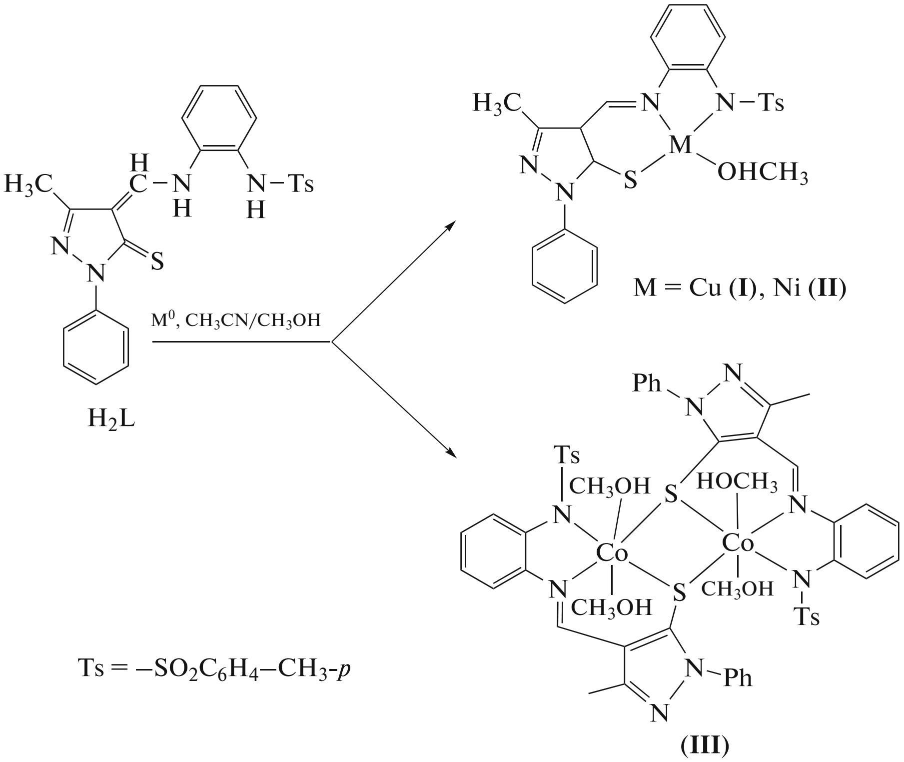

Scheme.

The electrochemical oxidation of cobalt, nickel, and copper used as anodes in the presence of H_2L in a methanol–acetonitrile mixture affords mononuclear complexes $[ML \cdot CH_3OH]$ (M = Cu (**I**) and Ni (**II**)) and binuclear cobalt chelate $[Co_2L_2 \cdot 4CH_3OH]$ (L is the dianionic form). The overall complexation reaction occurring in the electrolytic cell can be written as follows:

$$(-)Pt/CH_3OH/CH_3CN + H_2L/M(+),$$
$$M = Ni, Co, Cu.$$

Electrochemical syntheses of nickel and copper complexes:

$$\text{Cathode: } H_2L + 2e \rightarrow L^{2-} + H_2$$
$$\text{Anode: } M(Ni, Cu) + L^{2-} + CH_3OH$$
$$\rightarrow [ML \cdot CH_3OH] + 2e;$$

Electrochemical synthesis of cobalt complex:

$$\text{Cathode: } 2H_2L + 4e \rightarrow 2L^{2-} + 2H_2$$
$$\text{Anode: } 2Co + 2L^{2-} + 4CH_3OH$$
$$\rightarrow [Co_2L_2 \cdot 4CH_3OH] + 4e.$$

According to the experimental IR and ^1H NMR data, the thioenamine form of H_2L is most stable both in solution and in the solid state (Scheme). The IR spectrum of H_2L exhibits an intense stretching vibration band at 1638 cm^{-1} for of the vinylogous thioamide group C(=S)–CH=CHN [21], a band at 3215 cm^{-1} characteristic of ν(N–H) stretching vibrations, and bands at 1324 and 1154 cm^{-1} corresponding to asymmetric and symmetric $\nu(SO_2)$ stretching modes of the tosyl moiety, respectively. The ^1H NMR spectrum shows doublets at 8.67 and 14.49 ppm for the CH and NH protons of the aminomethylene C*H*N*H* group, respectively, with vicinal spin–spin coupling constant $^3J = 12.4$ Hz.

The IR spectra of complexes **I–III**, in comparison with the spectra of uncoordinated azomethine H_2L, no longer contain the band at 3215 cm^{-1} corresponding to the ν(N–H) stretching mode of the tosylated amino group and the band at 1638 cm^{-1} for the vinylogous thioamide group C(=S)–CH=CHN. Instead, 1603, 1604, and 1606 cm^{-1} bands corresponding to the ν(C=N) stretching vibrations appear in the spectra of **I**, **II**, and **III**, respectively.

The doublets for the aminomethylene moiety disappear from the ^{1}H NMR spectrum of complex **II**, and a singlet for C*H*=N imino group proton appears at 8.86 ppm. In addition, the ^{1}H NMR spectrum of **II** exhibits signals of coordinated methanol: a doublet for the methyl group at 3.21 ppm with the vicinal constant ^3J = 6.7 Hz and a quartet for the hydroxyl proton at 4.05 ppm. Thus, the set of ^{1}H NMR and IR data provides the conclusion that the ligand in compounds **I**–**III** occurs in the bis-deprotonated (L^{2-}) thiol imine form. The MN_2O_nS coordination unit of **I**–**III** is formed by the imine nitrogen atom of the CH=N bond, tosylated amino group nitrogen, thiol sulfur atom, and oxygen atoms of the coordinated methanol (n = 1 for **I** and **II**; n = 4 for **III**).

The local atomic structure of complexes **I**–**III** was established by from *K*-edge XANES and EXAFS spectra of these compounds. Figure 1 shows the normalized Cu, Co, and Ni *K*-edge XANES spectra and their first derivatives dμ/d*E* for compounds **I**–**III**. All XANES spectra have the principal absorption peak *C* corresponding to the $1s \to 4p^*$ electron transitions and low-intensity pre-edge peaks *A*, which appear in the spectra mainly because of *p*–*d* mixing of metal ion AOs at low symmetry of its environment. As can be seen in Fig. 1, the XANES spectra of **I**–**III** have rather intense pre-edge peaks *A*, indicating low symmetry of the environment of absorbing atoms. It is also noteworthy that the intensity of the pre-edge peaks *A* decreases in the series Co–Ni–Cu as the *d*-shell of ions is being occupied. A low symmetry of the environment is also indicated by the form of the edge first derivatives, which have several peaks because of splitting of the vacant *p*-levels of the metal ion in the crystal field of the environment.

The quantitative characteristics of the local atomic structure of complexes **I**–**III** were derived from analysis of the *K*-edge EXAFS spectra. Figure. 1 shows the FTM of EXAFS of the complexes. The FTM of complexes **I** and **II** contain the principal peak at r = 1.55–1.57 Å; the peak has a shoulder on the longer distance side $r \approx$ 1.80 Å. In accordance with the presumptive model of the local atomic structure, this FTM peak corresponds to photoelectron wave scattering on the two nearest coordination spheres consisting of ligand nitrogen and/or oxygen and sulfur atoms. The FTM of cobalt complex **III** shows two principal peaks of approximately equal amplitude at r = 1.47 and 1.76 Å; also an intense peak that is absent in the other FTM of complexes **I** and **II** is present at r = 2.74 Å. The increase in the amplitude of the r = 1.76 Å peak corresponding to sulfur coordination may attest to the increase in the coordination number, while the peak at longer distances is caused by scattering on the neighboring cobalt atom. For this complex, a model of a sulfur-bridged dimer was proposed. Theoretical calculation of the EXAFS spectra of complexes **I**–**III** were used to identify the best models for the local atomic structure; minimization of the $\Re$-factor served as the criterion (Fig. 1, *3*).

Table 2. Parameters of the local atomic environment of metal ions in complexes **I**–**III** found by multisphere fitting of *K*-edge EXAFS spectra*

Compound	*N*	*R*, Å	σ^2, Å^2	Coordination sphere	$\Re$, %
I (Cu)	2.8	1.99	0.0040	N/O	3.7
	1	2.23	0.0040	S	
	2	1.90	0.0040	N/O	
II (Ni)	1	2.01	0.0040	O/N	3.2
	1	2.22	0.0045	S	
	2	1.95	0.0038	N	
III (Co)	2	2.21	0.0048	S	4.7
	1	3.18	0.0055	Co	

* *R* is interatomic distance, σ^2 is the Debye–Waller factor, $\Re$ is the quality of fit function.

The quantitative data on the local atomic structure in complexes **I**–**III** are given in Table 2. It follows from the Table that the nearest coordination spheres of copper and nickel complexes consist of three nitrogen/oxygen atoms at average distances of 1.99 (**I**) and 1.90–2.01 Å (**II**) and one sulfur atom at a distance of 2.22–2.23 Å. In the cobalt complex **III**, two ligand nitrogens are located at an average distance of 1.95 Å and two sulfur atoms are at a distance of 2.21 Å. The molecule of complex **III** has a dimeric structure with a Co···Co distance of 3.18 Å. The mononuclear structure of copper complex **I** is supported by the magnetic moment (μ_{ef}) of 1.87 μ_B close to the spin value. The diamagnetic nature (χ_g = –0.387) of nickel complex **II** implies a square geometry of the NiN_2OS chelate unit. The binuclear structure of complex **III** is confirmed by the results of magnetochemical measurements (μ_{eff} = 3.18 μ_B).

The conclusions about the local atomic environment of the copper ion in complex **I** are confirmed by X-ray diffraction data.

The structural unit of complex **I** is the $[Cu(L)(CH_3OH)]$ molecule (Fig. 2). The coordination polyhedron of copper is a tetrahedrally distorted square. The bis-deprotonated azomethine residue L^{2-} is coordinated to copper(II) in the tridentate fashion via the amine and azomethine nitrogen atoms (N(1) and N(2), respectively) and the S(2) atom of the pyrazolethiol moiety. The fourth coordination site is occupied by the O(3) atom of the methanol molecule.

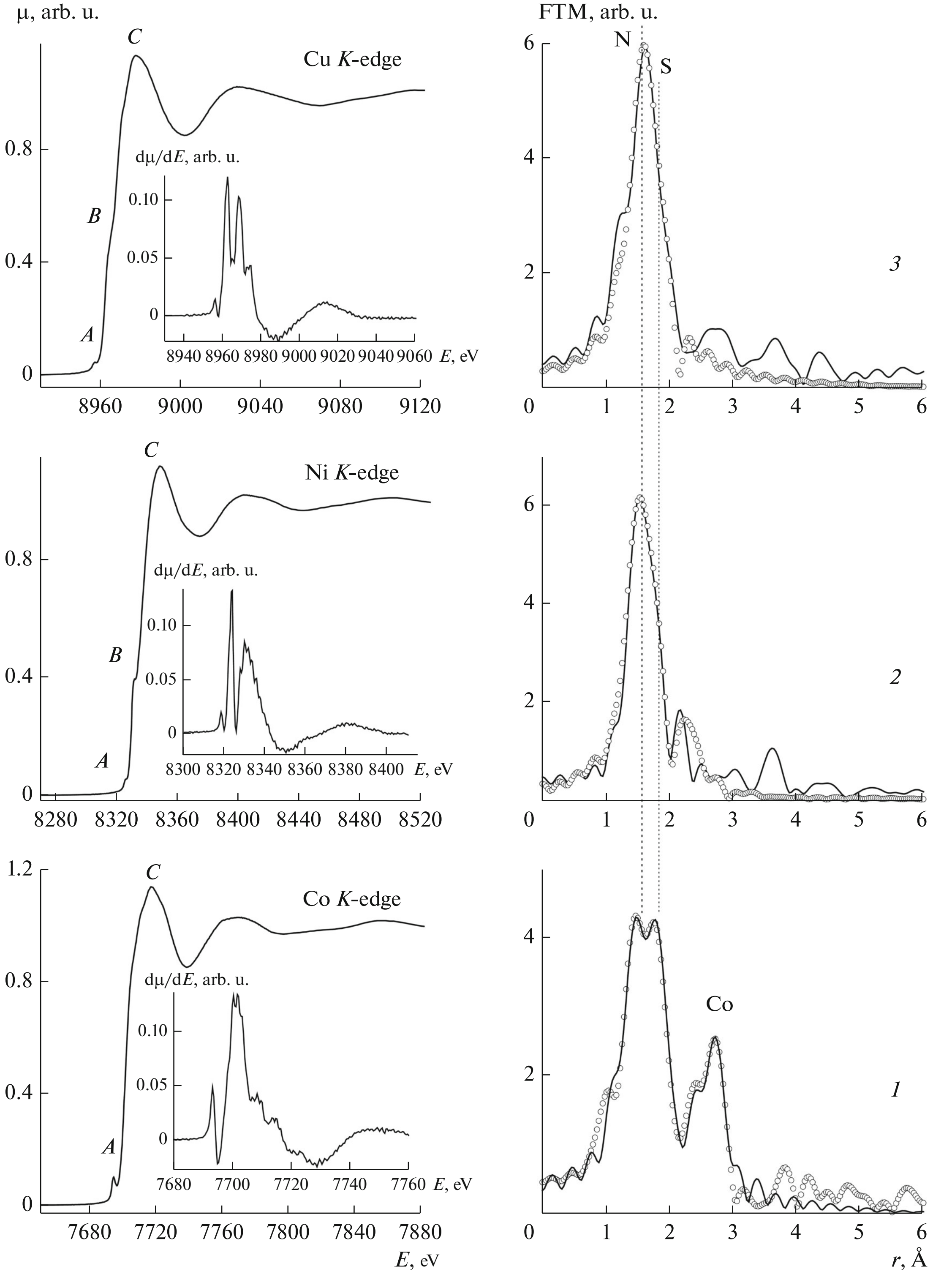

Fig. 1. Normalized XANES spectra (left panel), their first derivatives dμ/dE (inset), and EXAFS FTM (right panel) of (*1*) Co K-edge of **III**, (*2*) Ni K-edge of **II**, and (*3*) CuK-edge of **I**. The continuous line shows the experimental data and empty circles are theoretical results.

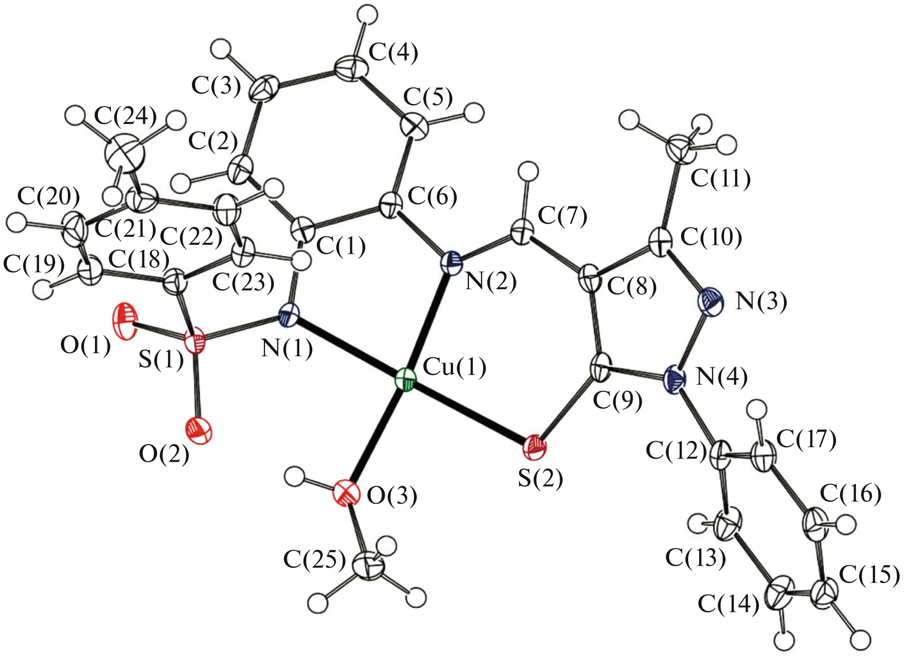

Fig. 2. Structure of a monomeric fragment of complex **I**. The atoms are represented as displacement ellipsoids at 50% probability level.

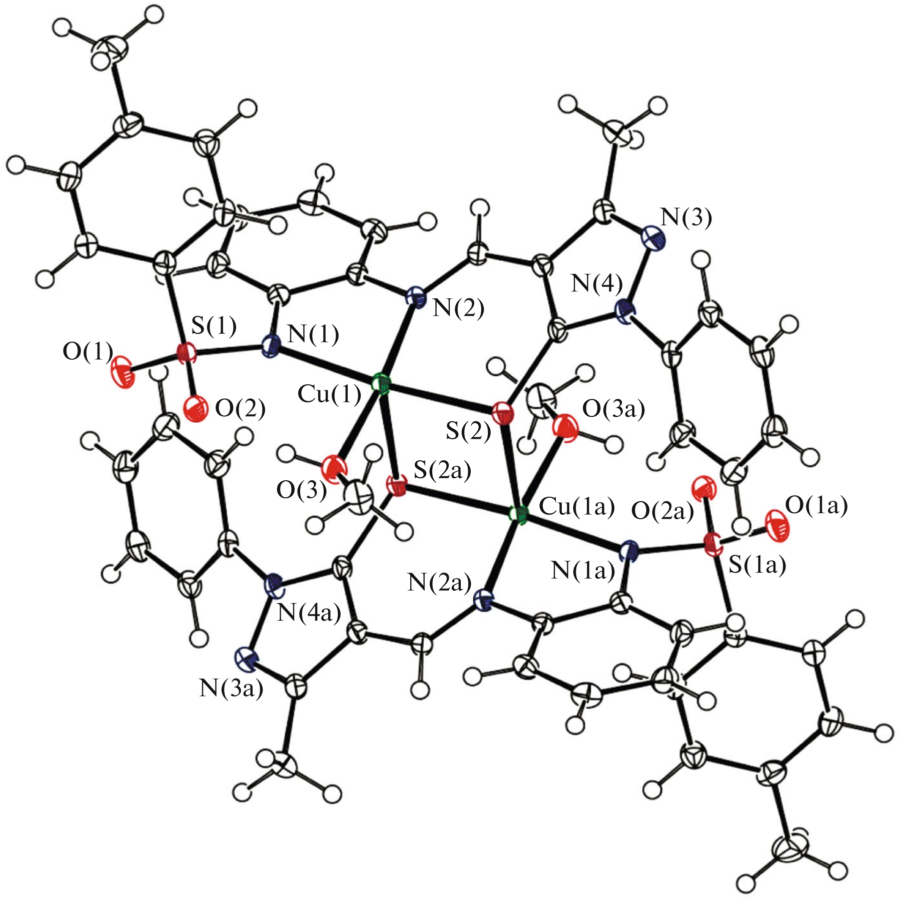

Fig. 3. Structure of a dimer of complex **I**. The atoms are represented as displacement ellipsoids at 50% probability level.

Table 3. Selected interatomic distances and bond angles in the copper coordination polyhedra of copper atoms in complex **I**

Bond	*d*, Å	Bond	*d*, Å
Cu(1)–N(2)	1.9534(18)	Cu(1)–N(1)	2.0688(19)
Cu(1)–O(3)	1.9979(17)	Cu(1)–S(2)	2.3038(6)
Angle	ω, deg	Angle	ω, deg
N(2)Cu(1)O(3)	174.14(8)	N(2)Cu(1)S(2)	97.23(6)
N(2)Cu(1)N(1)	81.92(8)	O(3)Cu(1)S(2)	88.57(6)
O(3)Cu(1)N(1)	92.22(7)	N(1)Cu(1)S(2)	171.65(5)

The azomethine ligand in the complex is generally non-planar. The phenyl group is substantially rotated relative to the pyrazole ring: the dihedral angle between the mean planes is 36.51°. The benzene ring of the tosylamine moiety is also non-coplanar with the pyrazole ring: the dihedral angle between the mean planes is 39.72°.

The five-membered chelate ring Cu(1)N(1)C(1)C(6)N(2) has an envelope conformation with the flap, Cu(1), being displaced from the mean plane through the other four atoms by 0.466 Å. The six-membered chelate ring Cu(1)N(2)C(7)C(8)C(9)S(2) also has an envelope conformation, the Cu(1) atom being located at a 0.494 Å distance from the mean plane through the other five atoms.

The methanol hydrogen atom forms an intramolecular hydrogen bond, O(3)–H(3)···O(2), with the O(2) atom of the tosyl moiety, the bond parameters being as follows: (O–H) 0.87, H···O 1.706, O···O 2.568(3) Å, ∠DHA 172°.

In the crystal of the complex, the Cu(1) atom forms a weak coordination bond with the $S(2)^i$ atom of the neighboring molecule, $Cu(1)–S(2)^i$, 2.9139(6) Å ($^i 1 - x, 1 - y, 1 - z$), which completes its coordination polyhedron to a highly elongated square pyramid (4 + 1) and gives rise to centrosymmetric dimers in which the bridging function is performed by S(2) atoms (Fig. 3, Table 3). The Cu(1)S(2)Cu(1a) bond angle is 83.97(2)°, the Cu(1)···Cu(1a) distance in the dimer is 3.5196(4) Å.

ACKNOWLEDGMENTS

The equipment of the Southern Federal University Collective Use Center “Molecular Spectroscopy” was utilized in the work.

This work was performed as a part of implementation of the Government Order for 2016 (no. 007-01114-16 PR 0256-2014-0009) and supported by the grant from President of the Russian Federation for the state support of leading scientific schools (NSh-8201.2016.3).

REFERENCES

1. Cassoux, P., Valade, L., and Fabre, P.-L., *Comprehensive Coordination Chemistry* II, Lever A.B.P., Ed., vol. 1, 2003, p. 761.
2. Rodríguez, A. and García-Vazquez, J.A., *Coord. Chem. Rev.*, 2015, vol. 303, p. 42.
3. Uraev, A.I., Vasilchenko, I.S., Ikorskii, V.N., et al., *Mendeleev Commun.*, 2005, vol. 15, no. 4, p. 133.
4. Bernal, M., García-Vazquez, J.A., Romero, J., et al., *Inorg. Chim. Acta*, 1999, vol. 295, no. 1, p. 39.
5. Garnovskii, A.D., Burlov, A.S., Garnovskii, D.A., et al., *Polyhedron*, 1999, vol. 18, no. 7, p. 1985.
6. Sanmartín, J., Novio, F., García-Deibe, A.M., et al., *Eur. J. Inorg. Chem.*, 2008, no. 10, p. 1719.
7. Garnovskii, D.A., Guedes da Silva, M.F.C., Kopylovich, M.N., et al., *Polyhedron*, 2003, vol. 22, no. 10, p. 1335.
8. Garnovskii, D.A., Sadikov, G.G., Antsyshkina, A.S., et al., *Cryst. Rep.*, 2003, vol. 48. no. 3., p. 426.
9. Sousa-Pedrares, A., Viqueira, J.A., Antelo, J., et al., *Eur. J. Inorg. Chem.*, 2011, no. 14, p. 2273.
10. Garnovskii, D.A., Antsyshkina, A.S., Sadikov, G.G., et al., *Russ. J. Inorg. Chem.*, 2014, vol. 59, no. 5, p. 431.
11. Garnovskii, D.A., Antsyshkina, A.S., Makarova, N.I., et al., *Russ. J. Inorg. Chem.*, 2015, vol. 60. no. 12, p. 1528.
12. Kvitko, I.Ya., *Zh. Org. Khim.*, 1969, vol. 5. no. 7, p. 1685.
13. Malick, W.U. and Sharma, T.S., *J. Ind. Chem. Soc.*, 1970, vol. 47, no. 2, p. 167.
14. Tuck, D.G., *Pure Appl. Chem.*, 1979, vol. 51, no. 10, p. 2005.
15. Chernyshov, A.A., Veligzhanin, A.A., Zubavichus, Y.V., et al., *Nucl. Instr. Meth. Phys. Res. A*, 2009, vol. 603, p. 95.
16. Kochubei, D.I., Babanov, Yu.A., Zamaraev, K.I., et al., *Rentgenospektral’nyi metod izucheniya struktury amorfnykh tel*: *EXAFS-spektroskopiya* (X-Ray Spectral Method for Investigation of Structures of Amorphous Bodies: EXAFS Spectroscopy), Novosibirsk: Nauka, Sib. otd., 1988.
17. Newville, M., J. *Synchrotron Rad.*, 2001, no. 8, p. 96.
18. Zabinsky, S.I., Rehr, J.J., Ankudinov, A., et al., *Phys. Rev. B*, 1995, vol. 52, p. 2995.
19. CrysAlisPro, Agilent Technologies. Version 1.171.36.32. Release 02-08-2013.
20. Sheldrick, G.M., *Program for the Refinement of Crystal Structure*, Göttingen: Univ. of Göttingen, 1997.
21. Kurkovskaya L.N., Shapet’ko N.N., Kvitko, I.Ya., et al., *Zh. Org. Khim.*, 1974, vol. 10. no. 10, p. 2210.

Translated by Z. Svitanko